From Nano Scale Silver Particles to Metallic Bulk Sizes: Increase of Silver Ion Reduction Rate in Chitosan:$AgNO_3$ Polymer electrolyte Mediated by Titanium Dioxide Filler

Shujahadeen B. Aziz[1,2*], Wrya O. Kareem[3], Hiwa O. Ghareeb[4]

[1]Prof. Hameeds Advanced Polymeric Materials Research Lab., Department of Physics, College of Science, University of Sulaimani, Qlyasan Street, Sulaimani, Kurdistan Regional Government-Iraq
[2]Komar Research Center (KRC), Komar University of Science and Technology, Sulaimani, 46001, Kurdistan Regional Government, Iraq
[3,4]Department of Chemistry, College of Science, University of Sulaimani, Qlyasan Street, Sulaimani, Kurdistan Regional Government-Iraq
* Corresponding Author: shujaadeen78@yahoo.com, shujahadeenaziz@gmail.com

Abstract: Synthesis of silver ion conducting polymer composites and its optical, electrical and morphological properties were conducted. In the study various amounts of titanium dioxide (TiO_2) was added to the chitosan:silver nitrate (CS:AgNt) system. The appearance of SPR peak for CS:AgNt system and CS:AgNt doped with 1 wt.% TiO_2 and disappearance of SPR peak for the system incorporated with 5 wt.% TiO_2 reveals the formation of silver particle from nano scales to bulk metallic sizes. The optical microscope images reveal the formation of silver particles with bulk metallic sizes at 5 wt.% TiO_2 filler . The SEM images show silver particles with small sizes for CS:AgNt and CS:AgNt incorporated with 1 wt.% TiO_2. To make sure the reduction process of silver ions to metallic silver particles the impedance spectroscopy has been carried out. The decrease of dielectric constant and DC conductivity at high TiO_2 concentration was correlated with the results of UV-vis and morphological achievments. Shifting of tanδ loss peak towards the lower frequency side at 5 wt.% TiO_2 is an evident for the decrease in conductivity. The results of the present work reveals that silver ion conducting polymer electrolytes mediated by TiO_2 filler are not suitable for electrochemical device application. Distinct peaks become visible in Mi spectra whereas no peaks can be seen in dielectric loss spectra.

Keywords: chitosan polymer composite; silver nanoparticle; Uv-vis study; Morphological study; electrical properties

1. Introduction

Solid polymer electrolyte (SPE) is expected to be employed as an alternative of the conventional organic sol–gel electrolyte in the near future due to its dimensional durability, processability, flexibility, electrochemical stability, safety and relatively long life time [1]. Since 1970s, a great attention has been devoted to the study of solid polymeric electrolytes. It is worth-mentioning that the measurements of the ionic conductivity in the polymer salt mixtures reported by Wright and coworkers and the development of ionic conductivity of polymer salt complexes by Armand and coworkers has occupied the literature for this topic [2]. Biopolymer-based films show promising potential as component of petroleum-based plastic package films in an attempt to minmise this detrimental environmental impact. The superior of film preparations from natural biopolymers over the artificial ones are; biodegradability, non-toxicity and edibility and in addition to these, some of them are effective barriers to oxygen and carbon dioxide due to their tightly packed, ordered

hydrogen-bonded network structure [3, 4]. Chitosan, a principal derivative of chitin, is a natural polymer, with low-cost and a weak alkalinity. A chitosan membrane can retain its chemical and thermal stability up to 200°C with a plausible mechanical strength. Furthermore, the existence of hydroxyl and amino groups on the backbone of chitosan make the chitosan membrane to be of a higher level of hydrophilicity, which is crucial for the operation of polymer electrolyte membrane fuel cells [5, 6]. Moreover, the removal of mercury from solutions and the adsorption kinetics of mercuric ions (Hg^{2+}) by chitosan were reported in literature [7]. Recently, it was reported that silver polymer electrolytes comprising silver salts dissolved in a polar polymer such as poly (2-ethyl-2-oxazoline) (POZ), poly (vinylpyrrolidone) (PVP) or poly (ethylene oxide) (PEO) matrix have attracted much attention for their application in solid state facilitated transport membranes. These silver SPEs have many advantages, including high separation performance, simple operation and low energy consumption [8-11]. The performance of the separation of olefin/paraffin mixtures by facilitated transport membranes containing silver salts is a promising alternative to energy-intensive distillation processes and as a consequence has attracted considerable interest [12]. It is well reported that lone pair electrons on atoms of functional groups of polar polymers are responsible for complexation with as well as reduction of silver ions [13-17]. A number of approaches have been proposed to solve the state-of-the-art problems of ion-conducting polymers. Among them, nanocomposite fabrication is the newest one [18]. It was confirmed that the incorporation of inorganic fillers such as SiO_2, α-Al_2O_3, $AlBr_3$, TiO_2 and ZnO into polymer electrolytes can enhance the mechanical stability and increase the conductivity due to higher polymer chain mobility and thus a faster cation diffusion [19, 20]. The noticeable data results of the present work reveals that the process of reduction of silver ions to nanoparticles in silver ion conducting polymer electrolyte membranes is a considerable challenging facing the purification and separation technologies using polymer membranes incorporated with silver ions. The data results of the present work shows that silver particles from nano scale to metallic bulk sizes occurred when a high amounts of TiO_2 filler has been added to the chitosan:AgNt electrolyte system. The reduction of silver ions to metallic silver particles has greatly affected the electrical properties of the composite samples as a result of charge carrying by ions rather than electron.

2. Experimental details

2.1. Sample Preparation

Chitosan from crab shells (≥75% deacetylated, average molecular weight 1.1×10^5, procured from Sigma), silver nitrate ($AgNO_3$) and Titanium dioxide (TiO_2, size < 100 nm) were purchased from sigma Aldrich. Acetic acid (1%) was prepared using glacial acetic acid solution that then used as a solvent medium in the preparation of the nanocomposite solid polymer electrolytes. The silver ion conducting films were syntheised by the solution cast technique. The preparation involved weighing 1 gm of chitosan (CS) and then dissolved in 100 ml of 1 % acetic acid solution. The mixture was stirred vigorously with a magnetic stirrer for several hours at room temperature until the chitosan powder has completely dissolved in the acetic acid solution. To this solution, 15 wt. % $AgNO_3$ was added with continuous stirring until homogeneous solution was obtained. To prepare nano-composite polymer electrolytes, initially the TiO_2 filler were first dispersed in 20 ml acetic acid solution with stirring. The TiO_2 concentrations were varied from 1 % up to 5 wt.%. The TiO_2 dispersions were mixed with the solutions of chitosan:$AgNO_3$ (CS:AgNt) and then continuously stirred. The solutions were then casted into different clean and dry Petri dish and allowed at room temperature until solvent-free films were obtained. The films were kept in desiccators with blue silica gel desiccant for further drying. The samples were coded as CSC 0, CSC 1 and CSC 2 for CS:AgNt incorporation with 0 wt.%, 1 wt.% and 5wt.% of TiO_2 filler, respectively.

2.2. Characterization Techniques

The nanaparticle formation was evidenced by the Uv-Visible spectra of the prepared films were recorded using a Jasco V-570, Uv-Vis-NIR spectrophotometer (Jasco SLM-468, Japan) in the

absorbance mode, and in the wavelength range of 190-1500 nm. The impedance of the samples was measured using the HIOKI 3531-Z Hi-tester in the frequency range 50 Hz - 1 MHz at ambient temperature. The films were mounted on the conductivity holder with blocking stainless steel electrodes of diameter 2 cm. The optical micrograph images of the prepared nanocomposites films were realized by Optical Microscope. The image acquisitions of the samples were conducted using an optical microscope (MEIJI) hyphenated with digital camera and software from DINO-LITE at adjusted magnification. A scanning electron micrograph (SEM) was taken using the (FEI Quanta 200) field emission scanning electron microscope (FE-SEM) to show the morphological characteristics.

3. Results and Discussion

3.1. UV-vis Study

Figure 1 shows the absorption spectra for CS:AgNt and a series of composite samples. The surface plasmonic resonance (SPR) peak with a weak intensity can be observed for CS:AgNt sample. It is clear that at 1 wt.% of TiO_2, the intensity of SPR peak greatly enhanced whereas at 5 wt. % of TiO_2 the SPR peak disappeared. This can be related to the reduction of a huge amount of silver ions to silver particles in the former case. For the latter case, coagulation of silver nanoparticles was occurred, resulting in the bulk metallic formation which is completely different from the nano size in both chemical and physical behaviour. From literature, one can see that SPR peaks appeared strongly when silver particles exist within nano scale ranges. It has been noticed that silver nanoparticles and their clusters can exhibit a characteristic surface plasmonic resonance (SPR) band in the ultraviolet and visible region and their heights gives insight into the population of the nanoparticles [13,14, 21, 22]. The SPR phenomenon is resulted from the collective oscillation of the electrons in the valence band in response to the incident beam (i.e., plasmon excitations) [23]. Earlier studies emphased that the position of LSPR band can be manipulated through controlling the concentration, size, shape, and behavior of the metal nanoparticles as well as the dielectric behavior of the host materials [24, 25]. It is interesting to notice that the broad LSPR peaks than the sharper ones can be due to the larger size distribution of the nanoparticles and their neighboring effects [24, 26]. Among the wide variety of metal nanoparticles, considerable effort has been devoted in the synthesis controlling and the investigation of silver metal particles, because of their unique optical, electrical, and chemical properties [27]. During the past few decades, silver nanoparticles have attracted considerable interests due to of their potential applications, such as electromagnetic interference shielding, antibiocial medical device and surface-enhanced Raman scattering (SERS). It was well known that surface roughness is very important for SERS [28]. Moreover, silver nanoparticles have wide applications, such as quantum dots, miniaturized electronic devices and as catalysts for organic reactions [27].

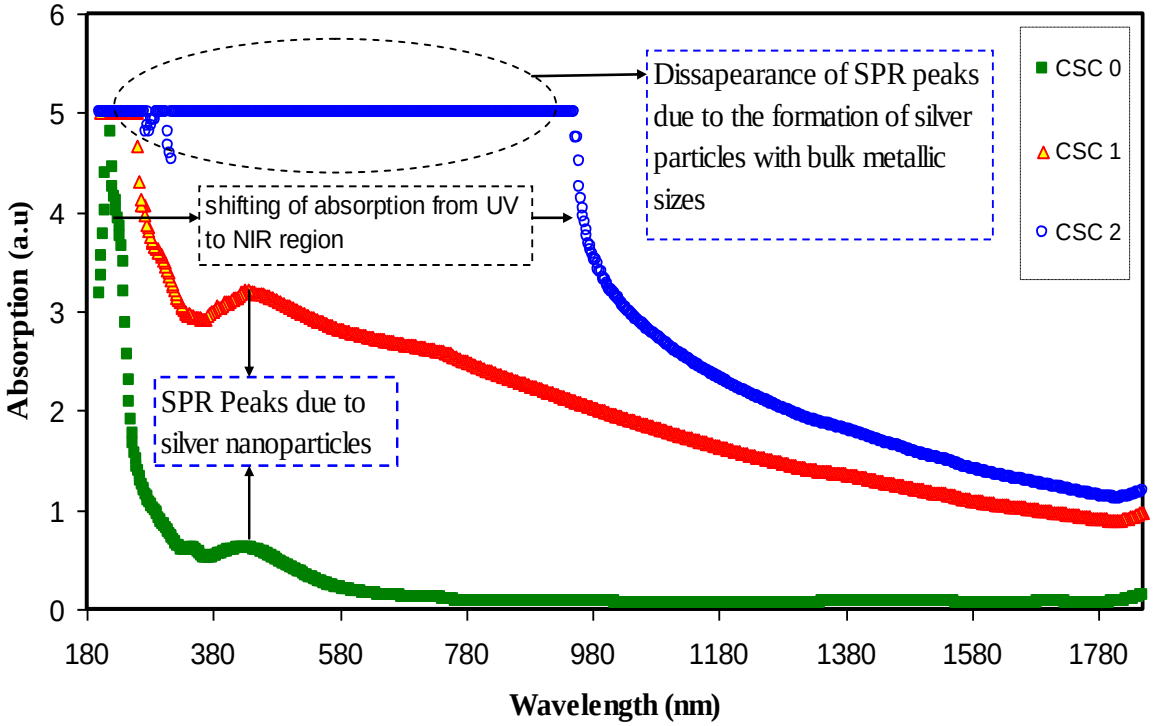

Figure 1. The UV-vis spectra for all the samples. the increase of SPR peak with increasing TiO_2 concentration is an evident for the increase of the amount of silver particles at 1 wt.TiO_2. the dissapearnce of SPR peak at 5 wt.% TiO_2 can be ascribed to the formation of silver particles with bulk metallic sizes. .

3.2. Morphological Study

Morphological studies may give more insights into the formation of silver particles with nano and bulk metallic sizes. **Figure 2** exhibits the optical micrograph (OM) for CS:AgNt and samples incorporated with various amounts of TiO_2 filler. From the image, one can observe clearly white spots with small sizes for CS:AgNt samples. The size and the number of white spots are increased with increasing the TiO_2 content. In the one hand, at 1 wt.% TiO_2, a massive number of discrete white spots can be observed on the surface of the sample. On the other hand, a large number of silver particles at 5 wt.% TiO (bulk metallic sized brilliant silver) was appeared. Both Uv-Vis spectra and morphological images support each others. The formation and growth of these white spots to larger size which was accelerated with increasing TiO_2 content reduces the effective number of silver ions (Ag^+) which is important for conduction and technological applications. Other researchers also observed the formation and growth of silver speaks in PEO-AgSCN complexes [29] and some other researchers used OM technique to observe the crystalline and amorphous phases. They have attributed the spherulites to the crystalline structure and dark regions to amorphous phase. Usually, the boundary between the spherulites is ascribed to the existence of amorphous phase [30]. The absence of spherulites in the samples of the present work reveals that CS:AgNt system and composite samples are amorphous. Clearly, only white specs with various sizes can be seen on the surface of the samples, for example, at 5 wt.% TiO_2, an obvious white chains of silver was appeared, indicating the formation of silver particles with bulk metallic sizes. Microscopic techniques, among them, scanning electron microscopy (SEM) are widely used to characterize the morphological appearance of solid and nanocomposites polymer electrolytes [14, 15, 31, 32].

Figure 3 shows the SEM images for all the samples. A huge number of silver specs with small sizes was observed on the surface of CS:AgNt samples. At 1 wt.% TiO_2, silver specs with large sizes are observed which can be related to the reduction of large amount of silver ions whereas at 5 wt.% TiO_2, silver particles aggregation can be seen. From these results, one can say that silver ion conducting polymer electrolytes incorporation with TiO_2 filler are not applicable for electrochemical

device applications and purification and separation of olefin/paraffin mixtures owing to the loss of silver ions.

Electrical studies may give more insights into the reduction of silver ions to metallic silver particles. Kang at al., studied the performance of POZ/$AgNO_3$ membrane with various amounts of SiO_2 incorporation instead of TiO_2 for separation of olefin/paraffin mixtures. It was observed that the membrane at 1 wt.% SiO_2 shows plausible facilitated olefin transport and enhancement of the selectivity of propylene/propane and propylene performance while at high silica concentration they observed poor separation performance for olefin/paraffin mixtures [8]. In their work, the light was not shed in the process of silver ion reduction. The study of the phenomena of reduction of silver ions to silver particles in silver ion polymer electrolyte membranes based on PEO was not performed by Sunderrajan et al. [33]. Liu et al., reported the gradual change in membrane performance with time, in the other word, stability test. They observed that conditioning of the membranes with permeant resulted in a decrease in the membrane performance, and such a change in membrane property was found to be irreversible. They achieved to the fact that continuous efforts must be given to investigate of the silver–PEO and silver–olefin interactions to gain a more understanding what causes the membrane instability in an attempt to develop appropriate approaches of improving the membrane durability [34]. Thus, the noticeable results of the present work reveals that the reduction of silver ions to nanoparticles in silver ion conducting polymer electrolyte membranes is the main difficulty facing the purification and separation technologies using polymer membranes incorporated with silver ions..

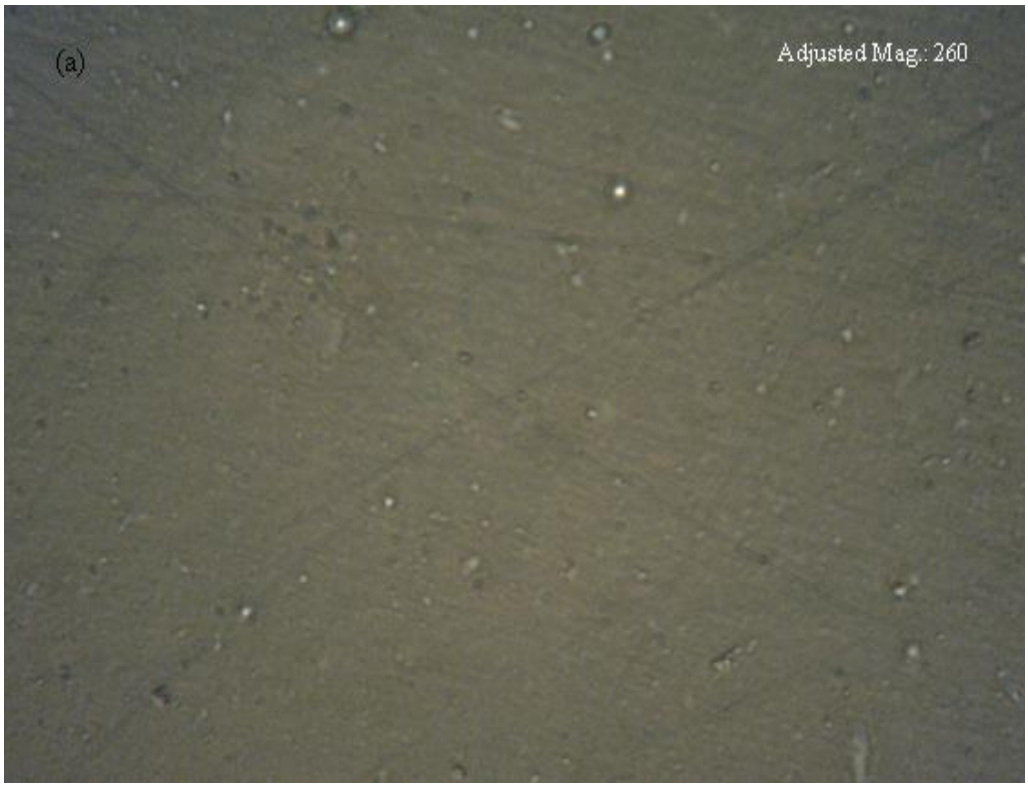

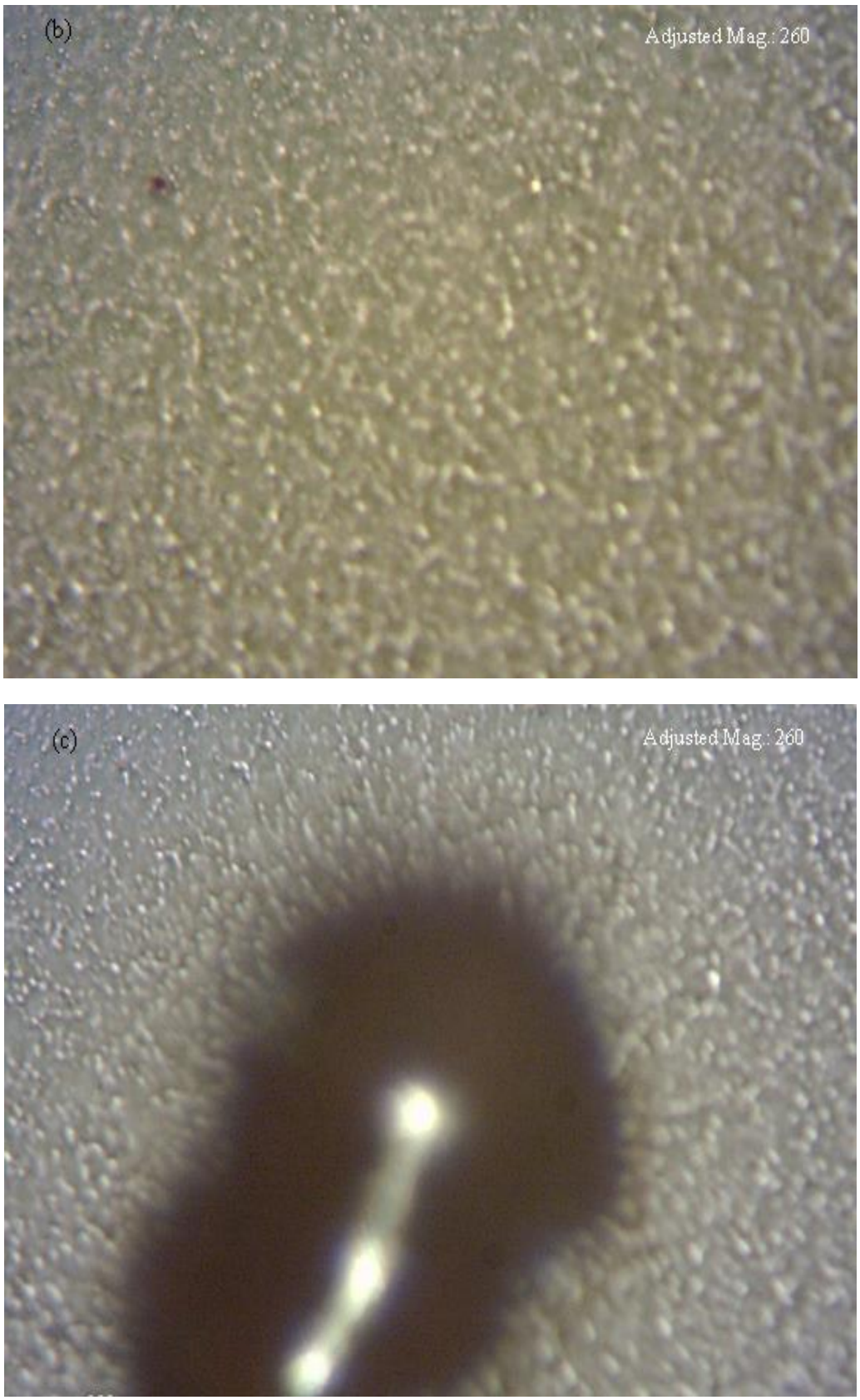

Figure 2. The OM images for (a) CSC0, (b) CSC 1 and (c) CSC 2 samples. Clearly silver particles from nano scale to bulk metallic sizes are appeared depending on the amount of the added TiO_2 filler.

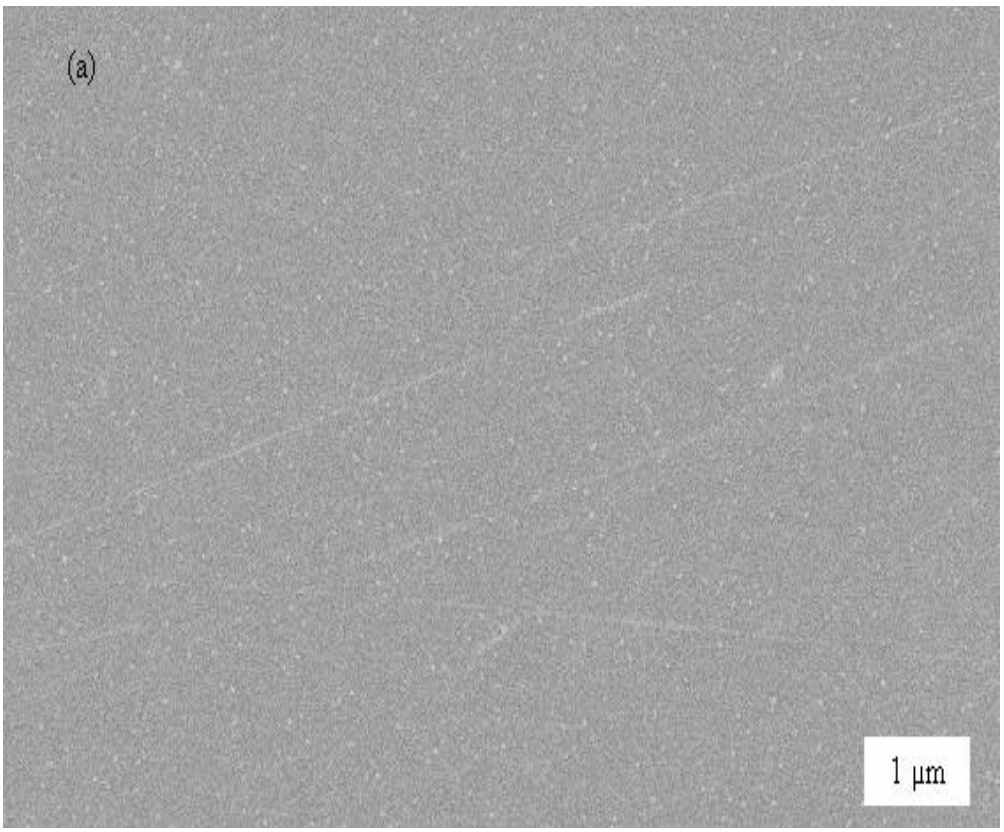

183

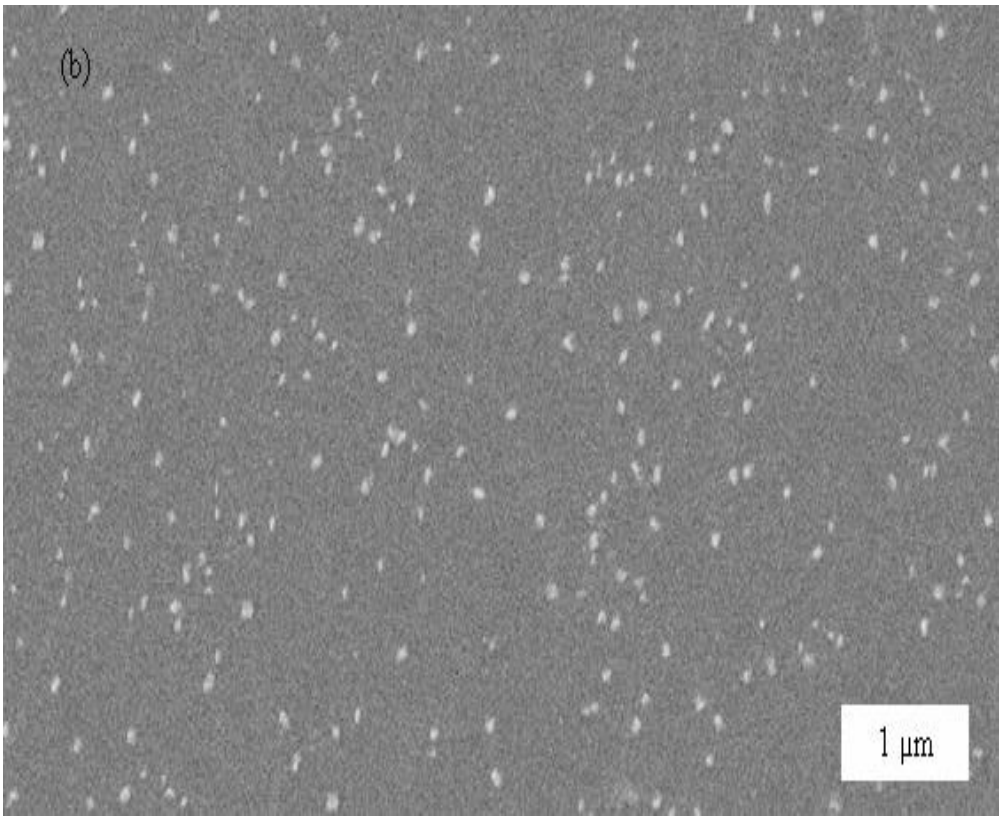

184

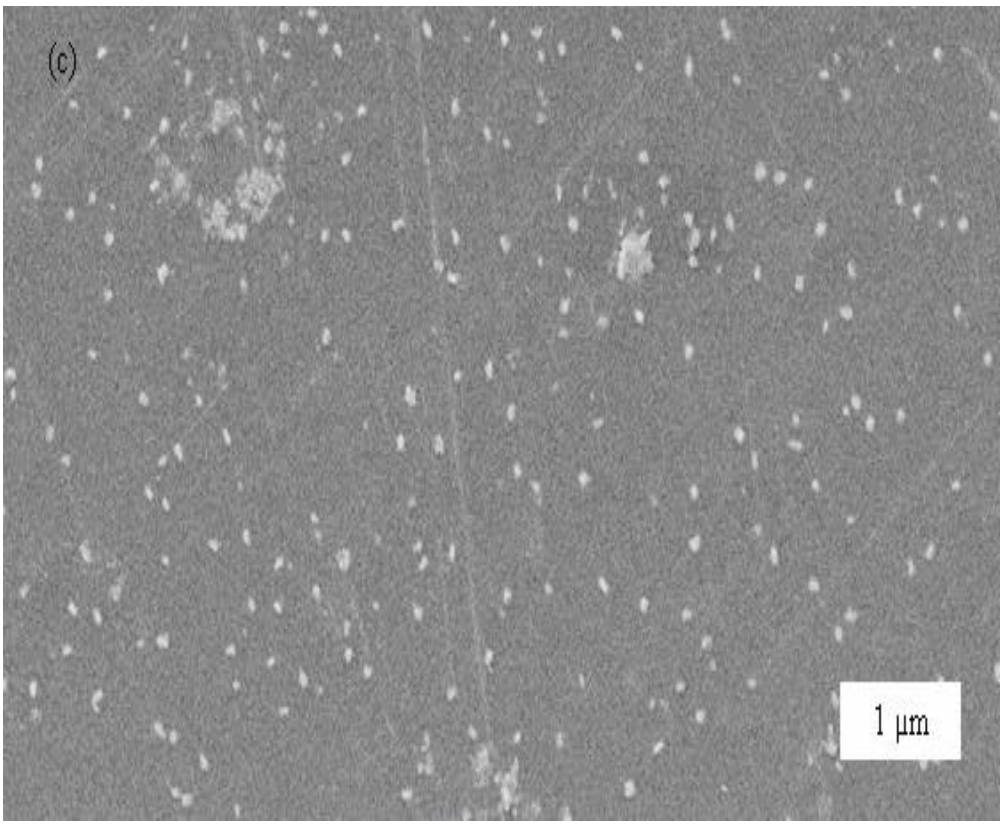

Figure 3. The SEM images for (a) CSC0, (b) CSC 1 and (c) CSC 2 samples. It is clear that the sizes of metallic silver particles are increase with increasing TiO_2 concentration.

3.3. Dielectric and electric modulus study

Here, a mathematical principle of impedance spectroscopy was shown. The real (Z_r) and imaginary (Z_i) part of complex impedance (Z^*) was also used for the evaluation of real and imaginary parts of dielectric and electric modulus using the following Equations [22, 35]:

$$\varepsilon' = \frac{Z_i}{\omega C_\circ (Z_r^{\,2} + Z_i^{\,2})} \quad (1)$$

$$\varepsilon'' = \frac{Z_r}{\omega C_\circ (Z_r^{\,2} + Z_i^{\,2})} \quad (2)$$

$$M' = \omega C_o Z_i \quad (3)$$

$$M'' = \omega C_o Z_r \quad (4)$$

Here, C_o is the vacuum capacitance and given by $\varepsilon_o A/t$, where ε_o is a permittivity of free space and is equal to 8.85×10^{-12} F/m. The angular frequency ω, is equal to $\omega = 2\pi f$, where f is the frequency of applied field.

Figure 4 and **5** exhibits the dielectric constant and dielectric loss respectively. Both the dielectric constant and dielectric loss decreased with increasing frequency to a minimum values at high frequency. The high values of these two properties were obtained from the charge accumulation at the electrode/electrolyte interface which in turn results in electrode polarization effects [6, 36]. The cause of dispersion of both values at low frequency is actually attributed to the contribution of charge accumulation at the electrode–electrolyte interface [37]. The values of dielectric constant at 10 kHz were presented in **Table 1**. The high dielectric constant returns back to CSC1 sample and the drop in

dielectric constant for CSC2 samples may be attributable to the reduction of huge amount of silver ions to silver particles and thus little silver ions remain to contribute in polarization as well as in conduction. Further supports for the phenomena of reduction of silver ions to silver particles may be grasped from the study of impedance plots and AC conductivity spectra as can be seen in the next sections. The absence of relaxation peaks in the dielectric loss spectra is due to the masking of polymer relaxation segments by DC ionic conductivity of ionic carriers [36, 38]. In polymer electrolytes with appreciable electrical conductivity, dielectric relaxation peaks due to permanent or induced dipoles may be masked by the relaxation from polarization of mobile charged species present in the material and thus the low frequency relaxation peaks cannot be appear as observed in the present work [39]. To gain understanding of the relaxation processes, tanδ was plotted as a function of frequency for all the samples as the tanδ shape in the **Figure 6** can be interpreted on the basis of Koops phenomenological model [40]. According to this model, loss tangent increases with an increase in frequency, and shows it's maximum value at particular frequencies for different temperatures because the ohmic component of current increases more rapidly than its capacitive component. At higher frequencies, loss tangent decreases with increasing frequency because the ohmic component of the current is virtually frequency independent and the capacitive component increases in proportion to frequency values [40, 41]. The broadness of the loss tangent peak indicates that the relaxation process is non-Debye relaxation [42].

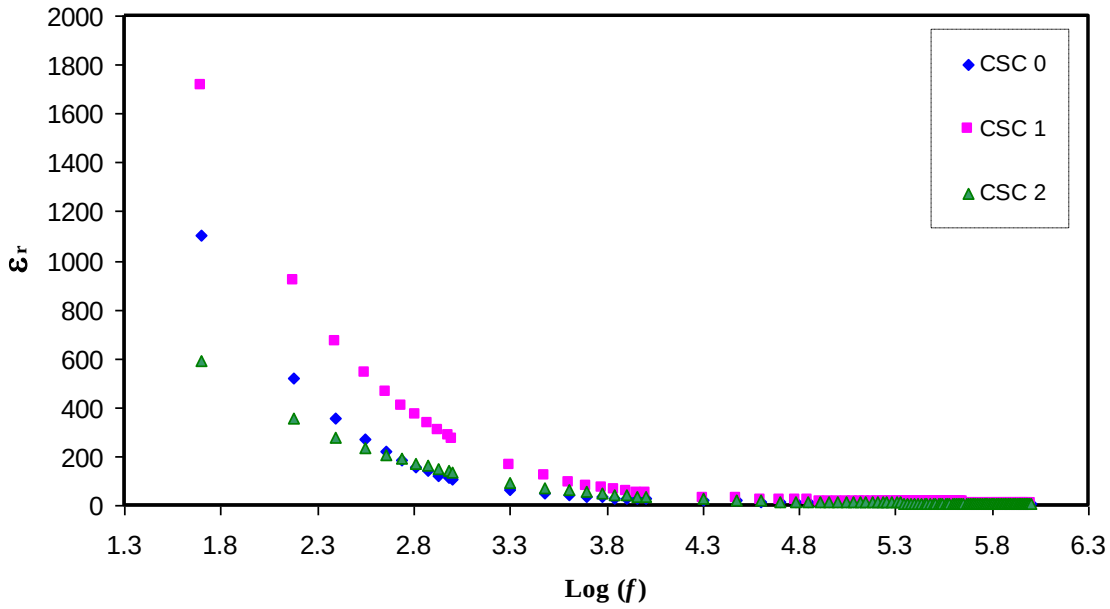

Figure 4 dielectric constant versus frequency for all the samples.

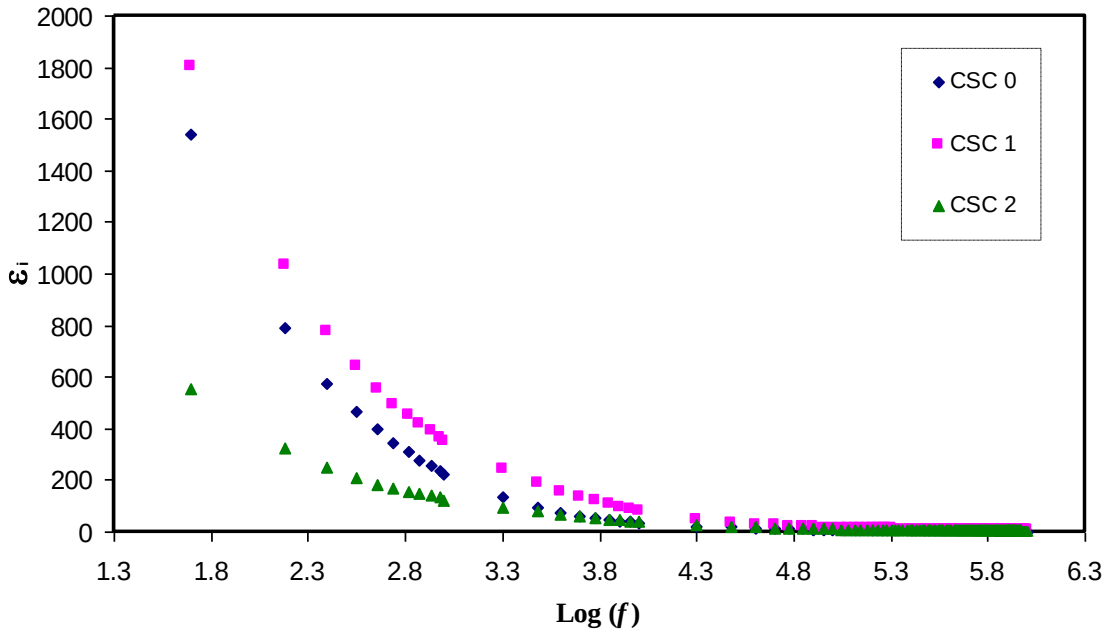

226

227 **F**igure 5 dielectric losses versus frequency for all the samples.

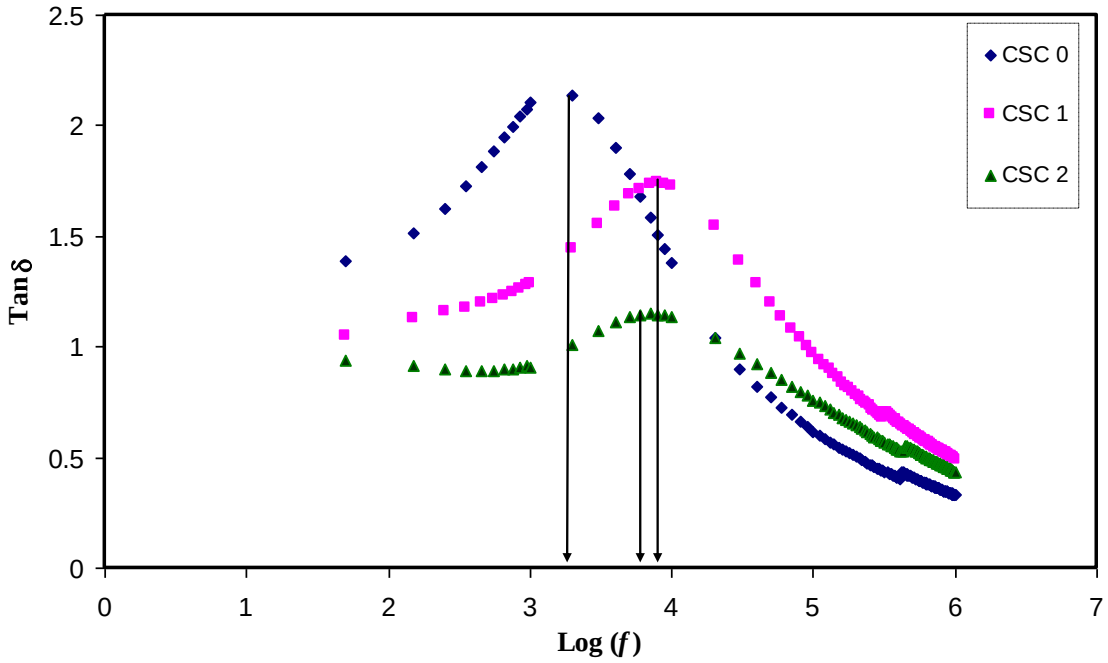

228

229 **F**igure 6 loss tangent versus frequency for all the samples.

230 **T**able 1 DC ionic conductivity and ε′ (at 10 kHz) for CS:AgNT sample and composite systems at
231 ambient temperature.

232

Sample Designation	Dielectric constant ε'	DC Conductivity (S/cm)
CSC0	26.53	4.67×10^{-7}
CSC1	47.34	1.18×10^{-6}
CSC2	35.51	4.87×10^{-7}

The dielectric response caused by ion relaxation has been studied using the reciprocal quantity of electric permittivity, known as the electric modulus in which the electrode polarization artifacts are suppressed. [43]. **Figures 7** and **8** show the real (M_r) and imaginary (Mi) parts of electric modulus respectively. The long tail observed in all the modulus spectra which can be ascribed to the suppression of low-frequency electrode/sample double layer impact arising due to their large capacitance values. In other words, the modulus spectral formalism has facilitated the process of idenfication and separation of electrode influence from the bulk relaxation phenomena occurring within it [44]. Distinguishable peaks are appeared in M_i spectra while these peaks are obscured in dielectric loss spectra (see Fig. 5). Previous studies confirmed that the dielectric loss (ε'') parameter always affected by an ohmic conduction (DC conductivity) [6, 35]. Consequently, the dielectric loss peaks are hidden in dielectric loss spectra as depicted in **Figure 5** and almost clearly appeared in M_i spectra (see **Figure 8**). From **Figure 8**, the distinguishable peaks in M″ spectra can also be observed and related to the conductivity relaxation. It is clear that with increasing TiO2 filler to 5 wt.% the relaxation peak shifted to the lower frequency side. This is related to the decrease of conductivity as a result of enormous amount of silver ion reduction. The peak present in the imaginary portion M_i identifies the regions where the carrier can move at long distance (left of the peak) or where the carrier are confined (right to the peak) [45].

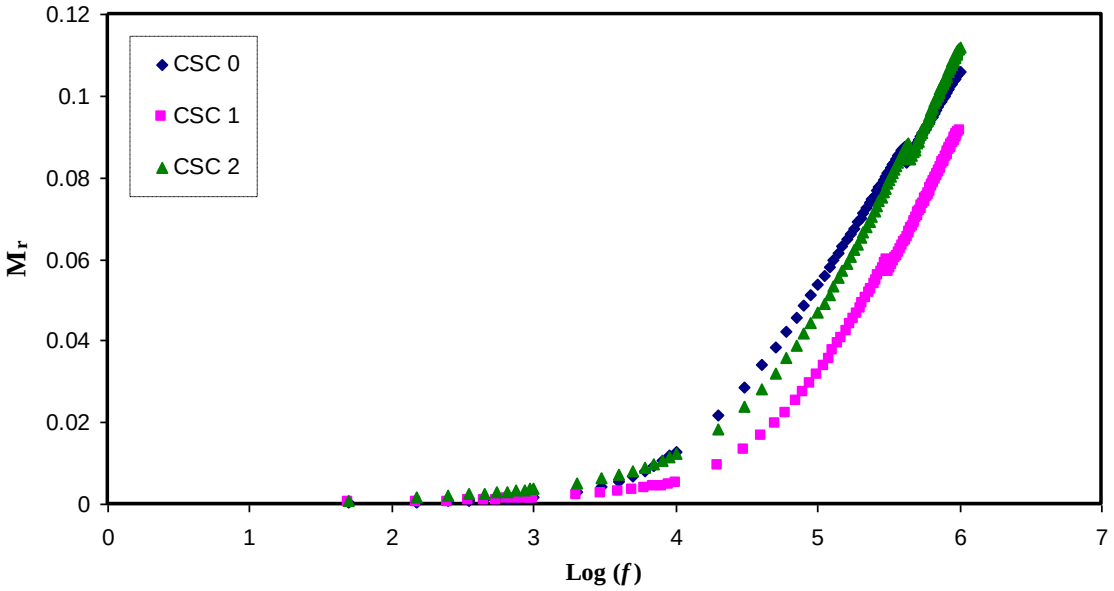

Figure 7 shows the M' value against frequency for all composite and CS:AgNt sample.

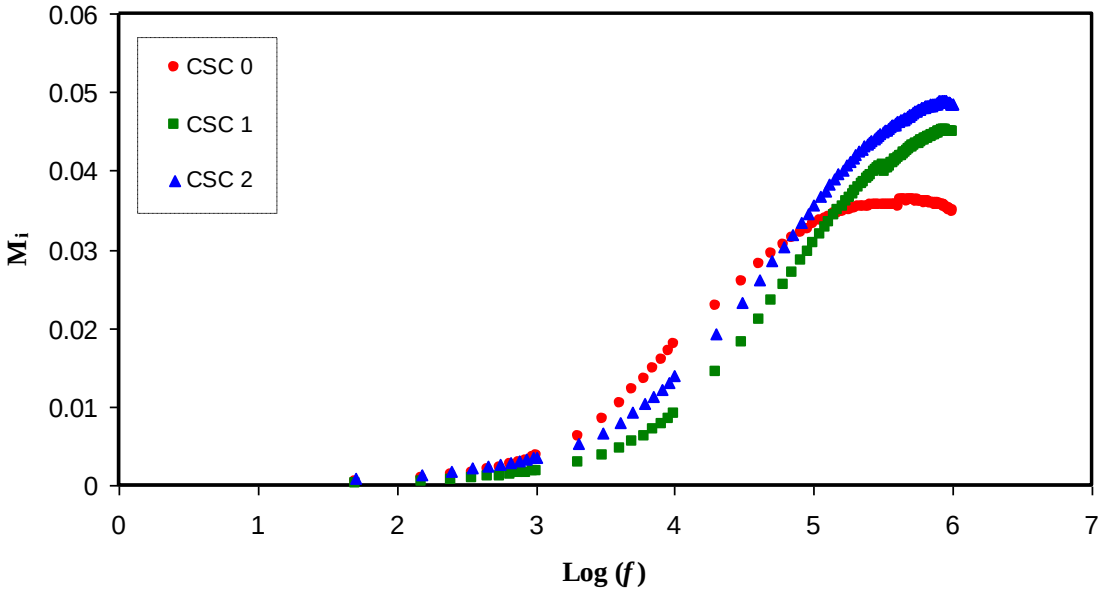

252

253 **F**igure 8 shows the M'' value against frequency for all composite and CS:AgNt sample.

254 *3.4. Impedance Study*

255 The understanding of charge transport mechanism in the composite materials is very important
256 both from fundamental and technological point of views. The impedance measurement is one of the
257 powerful techniques in the characterization and rationalization of the charge transport processes in
258 the complex materials [46]. Complex impedance plots (CIP) is a powerful tool in the analyzing the
259 electrical properties of polymeric materials that facilitates understanding structure–property
260 correlations [47]. **Figure 9** (a-c) exhibit the impedance plots for all the samples. Two distinct regions
261 at high and low frequencies can be observed clearly in the impedance spectra. The semicircle
262 observed in the high-frequency region is due to the bulk effect of the electrolytes and the linear region
263 in the low-frequency range can be attributed to the effect of the blocking electrode surfaces [48]. The
264 high frequency semicircle represents the bulk conductivity, which is due to the parallel combination
265 of both bulk resistance and bulk capacitance of the polymer electrolytes [49]. Since the blocking
266 electrodes have been used in the impedance analysis, the electrolyte/electrode interface could be
267 regarded as a capacitance like region. It is well-known that when the capacitance was ideal, it should
268 show a vertical spike in the impedance plot at low frequency region. However, the spike inclined at
269 an angle (y) with less than 90^{o} has been found instead of the vertical spike which may be related to
270 the roughness of the electrolyte/electrode interface or double layer capacitances at blocking electrodes
271 [50, 51]. The bulk resistance was extracted from the intercept of semicircle at high frequency with the
272 real axis of the impedance plot. This is associated to the fact that the complex impedance dominated
273 by the ionic conductance when the phase angle is close to zero [52]. The increase of bulk resistance
274 from 4 x 10^{3} Ohm for CSC1 system to 1.2 x 10^{3} Ohm for CSC2 system is related to the reduction of
275 enormous silver ions to silver particles (neutral silver in the form of particles). These silver particles
276 lost their ionic behavior and they act as grain boundaries. It is well reported that ion conducting
277 electrolytes are considered as the heart of electrochemical devises. Thus, silver ion conducting
278 electrolytes mediated by TiO_2 are not suitable for electrochemical applications including batteries and
279 super capacitors. The calculated DC conductivity from the bulk resistances were tabulated in **Table**
280 **1** showing the high DC conductivity for CSC1 sample. The decrease of DC conductivity for CSC2
281 samples is ascribed to the reduction of large amount of silver ions to silver particles at 5 wt.% TiO_2
282 and thereby little silver ions contributed to the DC conductivity.

283

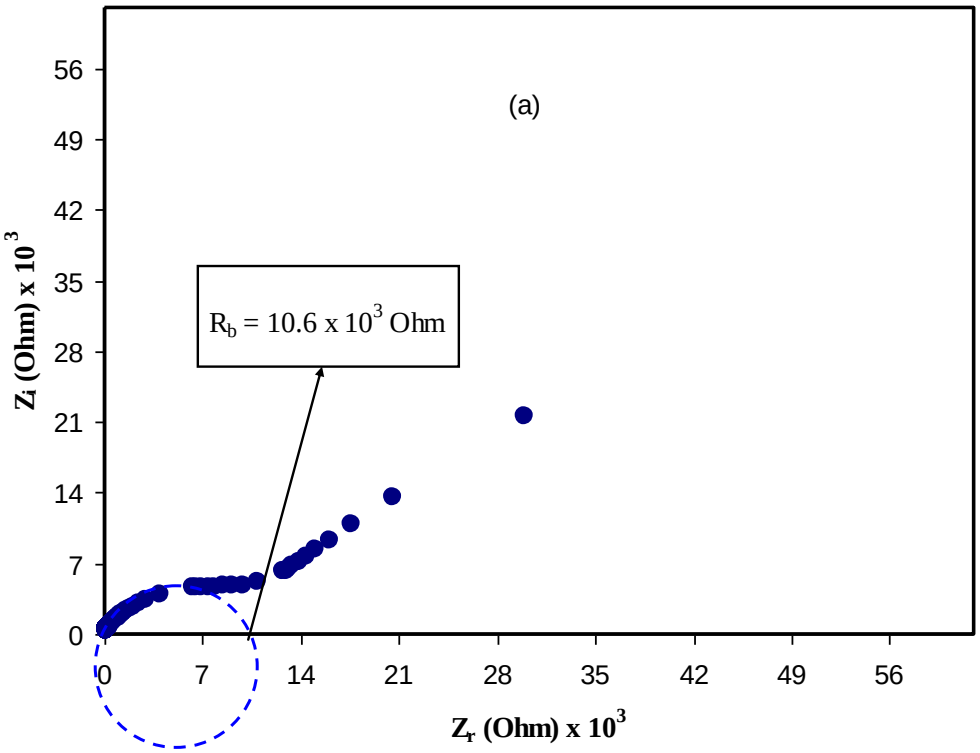
(a)
R_b = 10.6 x 10^3 Ohm
Z_i (Ohm) x 10^3
Z_r (Ohm) x 10^3
0
7
14
21
28
35
42
49
56

284

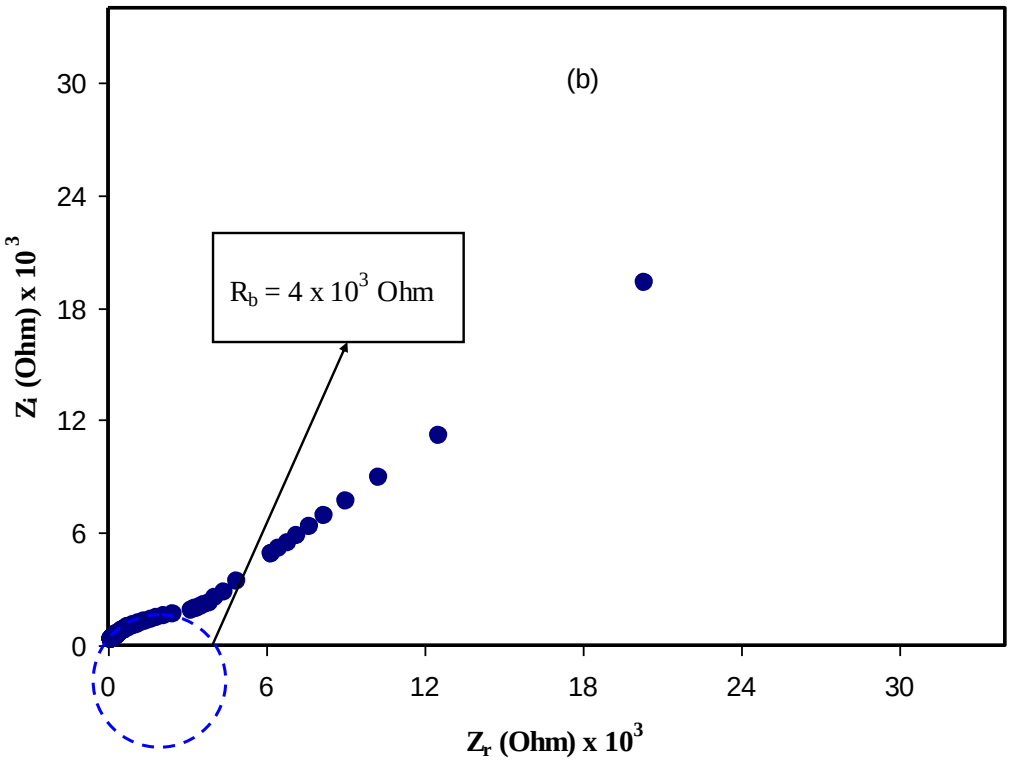
(b)
R_b = 4 x 10^3 Ohm
Z_i (Ohm) x 10^3
Z_r (Ohm) x 10^3
0
6
12
18
24
30

285

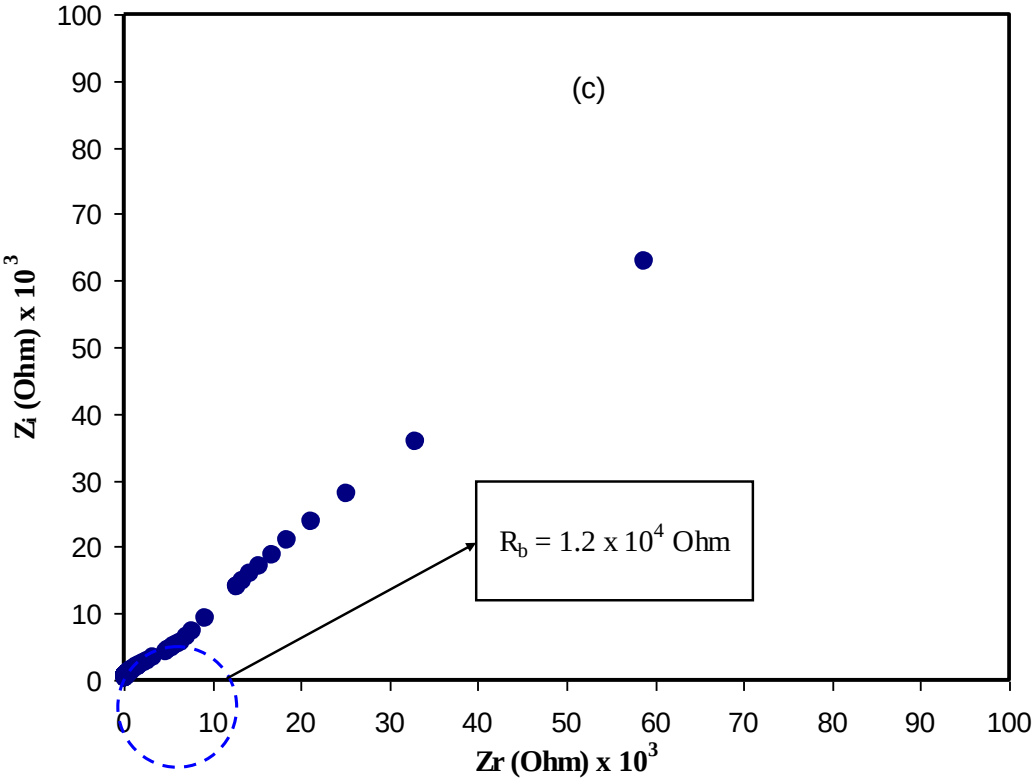

286

287 **F**igure 9 Impedance plots for (a) CSC 0, (b) CSC1 and (c) CSC2 composite samples at room
288 temperature.

289 *3.5. AC conductivity characterization*

290 **Figure 10** shows the AC conductivity (σ_{ac}) spectra for all the samples. It is well reported the
291 carrier transport properties of most materials could be investigated by measuring their ac and dc
292 electrical conductivities (σ_{ac} and σ_{dc}). The two types of conductivity are well related to each other
293 through the Jonscher empirical relation ($\sigma_{(\omega,T)} = \sigma_{ac} + \sigma_{dc}$) , where ω is the angular frequency of the
294 applied alternating electric field [53]. The onset frequency from which σ_{ac} starts to rise increases with
295 decreasing the capacitive reactance ($X_c = Z_i = 1/2\pi fC$). It is clear that at high frequency the capacitive
296 reactance is very low and thus most of the current passes through the capacitor element.
297 Consequently the σ_{ac} increases with increasing frequency and at high frequency region and exhibits
298 dispersion. Disordered solids are characterized by ac conductivity that varies as an approximate
299 power law of frequency [54]. According to Jonscher, the origin of frequency dependence of
300 conductivity lies in the relaxation phenomenon arising due to mobile charge carriers. The low
301 frequency spike can be associated to the electrode phenomena, especially at the interfacial region [13,
302 55, 56], while the frequency independent plateau region of the conductivity pattern corresponds to
303 dc conductivity of the material [57, 58]. The insets of Figure 10 show the DC conductivity value.
304 Compared to Table 1, the achieved DC conductivity from the AC spectra is in accordance with those
305 calculated from the impedance plots. Ion conducting electrolytes are considered as the heart of
306 electrochemical devices. Earlier studies revealed that prior of use of these electrolytes in the
307 electrochemical applications, such as battery and supercapacitor, their electrical properties must be
308 characterized [59]. In this regard, the decrease of DC conductivity upon increasing TiO2 filler has
309 shown the unsuitability of the current electrolytes for electrochemical applications. The Uv-Vis
310 studies and morphological appearances strongly supported the electrical results.

311

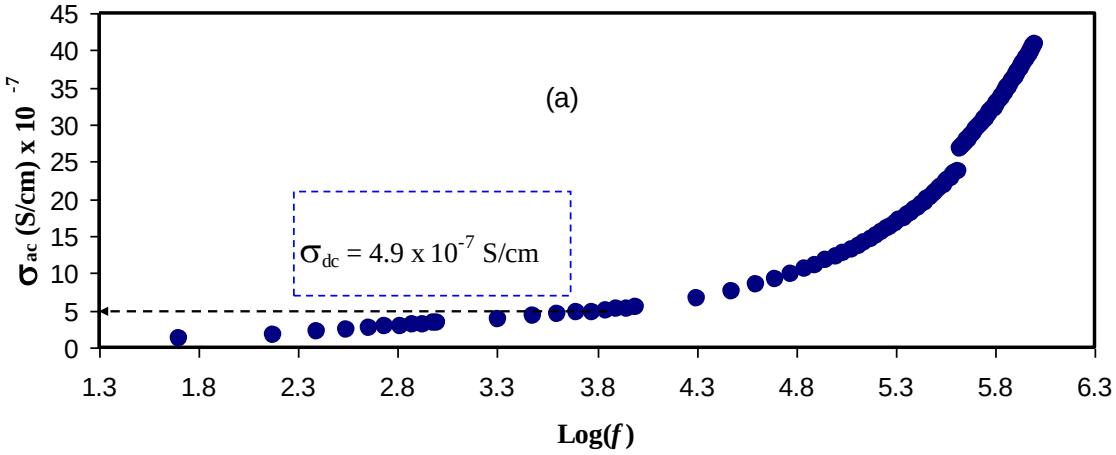

312

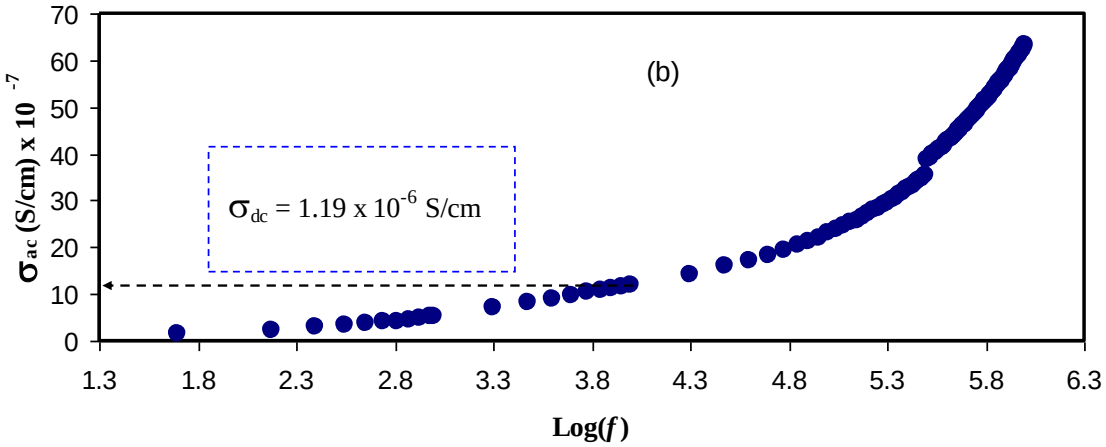

313

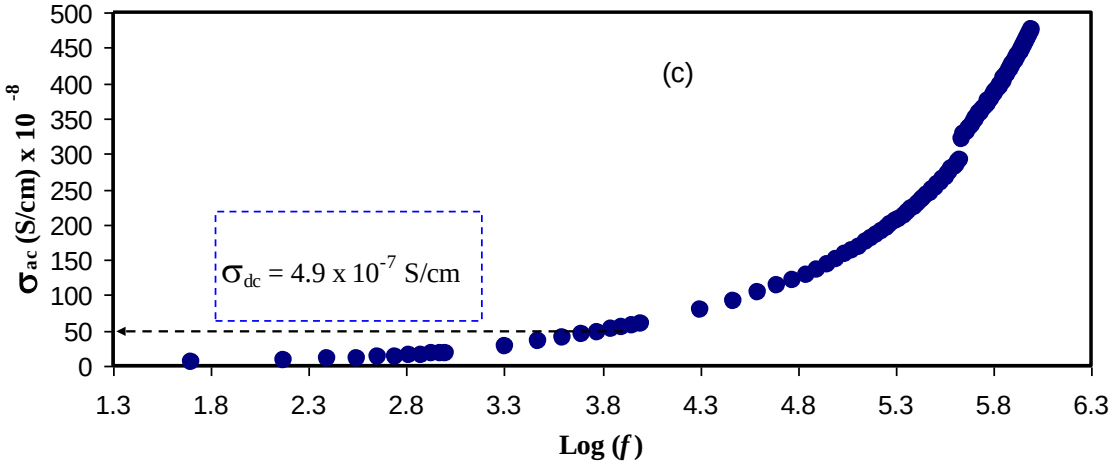

314

315 **Figure 10.** AC conductivity versus frequency for (a) CSC0, (b) CSC1 and (c) CSC2 sample at room
316 temperature.

317 **4. Conclusions**

318 In the conclusions, it is seemed that in the silver ion conducting polymer composites fabrication,
319 the concentration of TiO_2 has affected the mechanism of silver reduction process. The appearance
320 of SPR peak for CS:AgNt system and CS:AgNt doped with 1 wt.% TiO_2 indicates the formation of
321 silver nanoparticles. The increase of intensity and broadening of SPR peak at 1 wt.% TiO_2 can be
322 explained on the basis of the formation of huge amount of silver nanoparticles and the disappearance

of SPR peak for the system incorporated with 5 wt.% TiO_2 reveals the formation of silver particles with bulk metallic sizes.

The main conclusion of this work is that silver particles from nano scales to bulk metallic sizes can be fabricated in silver ion conducting chitiosan based electrolytes mediated by different concentration of TiO_2 filler. The optical microscope appearances reveal the formation of silver particles with bulk metallic sizes at 5 wt.% TiO_2 filler and percolation paths among silver particles can clearly be observed. To confirm the reduction of silver ions to metallic silver particles electrical impedance spectroscopy has been carried out. The decrease of dielectric constant at high TiO_2 concentration is an evident for the loose of silver ions. Shifting of tan loss peak towards the lower frequency side at 5 wt.% TiO_2 is a an evident for the decrease of conductivity. The drop in DC conductivity at high concentration of TiO_2 was explained based on the reduction of silver ions. The plateau in AC conductivity spectra was used to estimate the DC conductivity. The DC conductivity calculated from impedance plots are well agree with those achieved from the AC conductivity spectra. Finally, the work showed that silver ion conducting polymer electrolytes mediated by TiO_2 filler are not suitable for electrochemical device application as well as purification and separation of olefin/paraffin mixtures due to the loss of silver ions and formation of metallic silver particles. The long tails appeared in modulus spectra reveals the large capacitance associated with electrode polarization phenomenon. Distinct peaks become visible in Mi spectra whereas no peaks can be seen in dielectric loss spectra.

Acknowledgement: The authors gratefully acknowledge the financial support for this study from Ministry of Higher Education and Scientific Research-Kurdistan Regional Government, Department of Physics, College of Science, University of Sulaimani, Sulaimani, and Komar Research Center (KRC), Komar University of Science and Technology. The authors appreciatively acknowledge the financial support from the Kurdistan National Research Council (KNRC)- Ministry of Higher Education and Scientific Research-KRG, Iraq for this research project.

Author Contributions: Shujahadeen B. Aziz analyzed the data and wrote the paper. Wrya O. Kareem and Hiwa O. Ghareeb performed the experiments and reviewed the manuscript.

References

[1] M. Hema, S. Selvasekarapandian, D. Arunkumar, A. Sakunthala, H. Nithya "FTIR, XRD and ac impedance spectroscopic study on PVA based polymer electrolyte doped with NH4X (X = Cl, Br, I)" Journal of Non-Crystalline Solids 355 (2009) 84–90

[2] H. Nithya, S. Selvasekarapandian, D. Arun Kumar, A. Sakunthala, M. Hema, P. Christopherselvin, Junichi Kawamura, R. Baskaran, C. Sanjeeviraja "Thermal and dielectric studies of polymer electrolyte based on P(ECH-EO)" Materials Chemistry and Physics 126 (2011) 404-408

[3] Y. Li, X. Guo, P. Lin, C. Fan, Y. Song "Preparation and functional properties of blend films of gliadins and chitosan" Carbohydrate Polymers 81 (2010) 484–490

[4] N. S. Salleh, S. B. Aziz, Z. Aspanut, M. F. Z. Kadir "Electrical impedance and conduction mechanism analysis of biopolymer electrolytes based on methyl cellulose doped with ammonium iodide" Ionics 22 (2016) 2157–2167

[5] Y. Wan, B. Peppley, K. A.M. Creber, V. Tam Bui, Ela Halliop "Preliminary evaluation of an alkaline chitosan-based membrane fuel cell" Journal of Power Sources 162 (2006) 105–113

[6] S. B. Aziz "Occurrence of electrical percolation threshold and observation of phase transition in chitosan(1−x):AgIx (0.05 ≤ x ≤ 0.2)-based ion-conducting solid polymer composites" Applied Physics A 122 (2016) 706

[7] M. N.V. R. Kumar "A review of chitin and chitosan applications" Reactive & Functional Polymers 46 (2000) 1 –27

[8] S. W. Kang, J. H. Kim, K. Char, J. Won, Y. S. Kang "Nanocomposite silver polymer electrolytes as facilitated olefin transport membranes" Journal of Membrane Science 285 (2006) 102–107

[9] J. H. Kim, S. M. Park, J. Won, Y. S. Kang "Dependence of facilitated olefin transport on the thickness of silver polymer electrolyte membranes" Journal of Membrane Science 236 (2004) 209–212

[10] J. H. Kim, B. R. Min, H. S. Kim, J. Won,Y. S. Kang "Facilitated transport of ethylene across polymer membranes containing silver salt: effect of HBF4 on the photoreduction of silver ions" Journal of Membrane Science 212 (2003) 283–288

[11] S. H. Mun, S. W. Kang, J.-S. Cho, S.-K. Koh, Y. S. Kang "Enhanced olefin carrier activity of clean surface silver nanoparticles for facilitated transport membranes" Journal of Membrane Science 332 (2009) 1–5

[12] J. H. Kim, J. Won, Y. S. Kang "Olefin-induced dissolution of silver salts physically dispersed in inert polymers and their application to olefin/paraffin separation" Journal of Membrane Science 241 (2004) 403–407

[13] S. B. Aziz, R. M. Abdullah, M. A. Rasheed, H. M. Ahmed "Role of Ion Dissociation on DC Conductivity and Silver Nanoparticle Formation in PVA: AgNt Based Polymer Electrolytes: Deep Insights to Ion Transport Mechanism" Polymers 9 (2017) 338; doi:10.3390/polym9080338

[14] S. B. Aziz, Z. H. Z. Abidin, M. F. Z. Kadir "Innovative method to avoid the reduction of silver ions to silver nanoparticles ($Ag^{+} \rightarrow Ag^{o}$) in silver ion conducting based polymer electrolytes" Phys. Scr.90 (2015) 035808 (9pp)

[15] S. B. Aziz, O. Gh. Abdullah, M. A. Rasheed "A novel polymer composite with a small optical band gap: New approaches for photonics and optoelectronics" Journal of Applied Polymer Science 134 (2017) 44847

[16] S. B Aziz, M. A. Rasheed, Z. H. Z. Abidin "Optical and Electrical Characteristics of Silver Ion Conducting Nanocomposite Solid Polymer Electrolytes Based on Chitosan" Journal of Electronic Materials 46 (2017) 6119–6130

[17] S. W. Kang, J. H. Kim, K. S. Oh, J. Won, K. Char, H. S. Kim, Y. S. Kang "Highly stabilized silver polymer electrolytes and their application to facilitated olefin transport membranes" Journal of Membrane Science 236 (2004) 163–169

[18] S. R. Mohapatra, A. K. Thakur, R. N. P. Choudhary "Effect of nanoscopic confinement on improvement in ion conduction and stability properties of an intercalated polymer nanocomposite electrolyte for energy storage applications" Journal of Power Sources 191 (2009) 601–613

[19] T. Blensdorfa, A. Joenathana, M. Huntb, U. Werner-Zwanzigerc, B. D. Steind, W. E. Mahmoude, A. A. Al-Ghamdie, J. Carinif, L. M. Bronstein "Hybrid Composite Polymer Electrolytes: Ionic Liquid as a Magic Bullet for the Poly(ethylene glycol)-Silica Network" J. Mater. Chem A., 2016, 00, 1-3

[20] J. Shim, D.-G. Kim, H. J. Kim, J. H. Lee, J.-H. Baik, J.-C. Lee "A novel composite polymer electrolytes containing poly(ethylene glycol)-grafted graphene oxide for allsolid-state lithium-ion battery applications" Journal of Materials Chemistry A **2** (2014) 13873-13883

[21] S. B. Aziz, Z. H. Z Abidin, A. K. Arof "Effect of silver nanoparticles on the DC conductivity in chitosan–silver triflate polymer electrolyte" Physica B: Condensed Matter 405 (2010) 4429–4433

[22] S. B. Aziz, Z. H. Z Abidin, A. K. Arof "Influence of silver ion reduction on electrical modulus parameters of solid polymer electrolyte based on chitosan-silver triflate electrolyte membrane" Express Polym Lett 5 (2010) 300-310

[23] S. B. Aziz, R. T. Abdulwahid, H. A. Rsaul, H. M. Ahmed "In situ synthesis of CuS nanoparticle with a distinguishable SPR peak in NIR region" Journal of Materials Science: Materials in Electronics 27 (2016) 4163-4171

[24] S. B. Aziz, M. A. Rasheed, H. M. Ahmed "Synthesis of Polymer Nanocomposites Based on [Methyl Cellulose](1-x):(CuS)x ($0.02\ M \leq x \leq 0.08\ M$) with Desired Optical Band Gaps" Polymers 9 (2017) 193; doi: 10.3390/polym9060194

[25] L. V. Hong, D. T. Cat, L. H. Chi, N. T. Thuy, T. V. Hung, L. N. Tai, D. P. Long, "Plasmonic Effect in Au-Added TiO2-Based Solar Cell. J. Electron. Mater. 2016, 45, 4833–4837.

[26] G. Carotenuto, A. Longo, C. L. Hison, "Tuned linear optical properties of gold-polymer nanocomposites" J. Mater. Chem. 2009, 19, 5744–5750.

[27] D. G. Angelescu, M. Vasilescu, R. Somoghi, D. Donescu, V. S. Teodorescu "Kinetics and optical properties of the silver nanoparticles in aqueous L64 block copolymer solutions" Colloids and Surfaces A: Physicochem. Eng. Aspects 366 (2010) 155–162

[28] D.-G. Yu, W.-Ch. Lin, Ch.-H. Lin, L.-M. Chang, M.-C. Yang "An in situ reduction method for preparing silver/poly(vinyl alcohol) nanocomposite as surface-enhanced Raman scattering (SERS)-active substrates" Materials Chemistry and Physics 101 (2007) 93–98

[29] S. S. Sekhon, G. Singh, S. A. Agnihotry, S. Chandra "Solid polymer electrolytes based on polyethylene oxide-silver thiocyanate" Solid State Ionics 80 (1995) 37-44

[30] D. K. Pradhan, R. N. P. Choudhary, B. K. Samantaray "Studies of Dielectric Relaxation and AC Conductivity Behavior of Plasticized Polymer Nanocomposite Electrolytes" Int. J. Electrochem. Sci., 3 (2008) 597 - 608

[31] S. Ramesh, C.-W. Liew, E. Morris, R. Durairaj "Effect of PVC on ionic conductivity, crystallographic structural, morphological and thermal characterizations in PMMA–PVC blend-based polymer electrolytes" Thermochimica Acta 511 (2010) 140-146

[32] D. Wei, W. Sun, W. Qian, Y. Ye, X. Ma, "The synthesis of chitosan-based silver nanoparticles and their antibacterial activity", Carbohyd Res 344 (2009) 2375-2382

[33] S. Sunderrajan, B. D. Freeman, C. K. Hall, I. Pinnau "Propane and propylene sorption in solid polymer electrolytes based on poly(ethylene oxide) and silver salts" Journal of Membrane Science 182 (2001) 1–12

[34] L. Liu, X. Feng, A. Chakma "Unusual behavior of poly(ethylene oxide)/AgBF4 polymer electrolyte membranes for olefin–paraffin separation" Separation and Purification Technology 38 (2004) 255–263

[35] S. B. Aziz "Study of electrical percolation phenomenon from the dielectric and electric modulus analysis" Bulletin of Materials Science 38 (2015) 1597–1602

[36] S. B. Aziz, Z. H. Z. Abidin "Ion-transport study in nanocomposite solid polymer electrolytes based on chitosan: Electrical and dielectric analysis" J. Appl. Polym. Sci. 132 (2015) 41774

[37] R. Baskaran, S. Selvasekarapandian, G. Hirankumar, M.S. Bhuvaneswari "Vibrational, ac impedance and dielectric spectroscopic studies of poly(vinylacetate)–N,N–dimethylformamide–LiClO4polymer gel electrolytes" Journal of Power Sources 134 (2004) 235–240

[38] S. B. Aziz "Li^+ ion conduction mechanism in poly (ε-caprolactone)-based polymer electrolyte" Iranian Polymer Journal 22 (2013) 877–883

[39] P. A. R. D. Jayathilaka, M. A. K. L. Dissanayake, I. Albinsson, B.-E. Mellander, Solid State Ionics, 156 (2003) 179-195

[40] P. Khatri, B. Behera, V. Srinivas, R. P. N. Choudhary, Current Applied Physics, 9 (2009) 515-519

[41] B. Louati, F. Hlel, K. Guidara, Journal of Alloys and Compound 486 (2009) 299-303

[42] N. H. Idris, H. B. and Senin, A. K. Arof, Ionics, 13 (2007) 213-217

[43] C. S. Ramya, S. Selvasekarapandian, G. Hirankumar, T. Savitha, P.C. Angelo "Investigation on dielectric relaxations of PVP–NH4SCN polymer electrolyte" Journal of Non-Crystalline Solids 354 (2008) 1494–1502

[44] S. A. Suthanthiraraj, D. J. Sheeba, B. J. Paul "Impact of ethylene carbonate on ion transport characteristics of PVdF–AgCF3SO3 polymer electrolyte system" Materials Research Bulletin 44 (2009) 1534–1539

[45] A. Patsidis, G. C. Psarras, "Dielectric behaviour and functionality of polymer matrix–ceramic BaTiO3 composites" eXPRESS Polym. Lett. 2 (2008) 718-726

[46] T. Machappa, M. V. N. A. Prasad "AC conductivity and dielectric behavior of polyaniline/sodium metavenadate (PANI/NaVO3) composites" Physica B 404 (2009) 4168 –4172

[47] C. Justin Raj, K. B. R. Varma " Synthesis and electrical properties of the (PVA) 0.7(KI)0.3·xH2SO4(0≤x≤ 5) polymer electrolytes and their performance in a primary Zn/MnO2battery" Electrochimica Acta 56 (2010) 649–656

[48] S. Selvasekarapandian, R. Baskaran, M. Hema ""Complex AC impedance, transference number and vibrational spectroscopy studies of proton conducting PVAc–NH4SCN polymer electrolytes" Physica B 357 (2005) 412– 419

[49] J. Malathi, M. Kumaravadivel, G.M. Brahmanandhan, M. Hema, R. Baskaran, S. Selvasekarapandian "Structural, thermal and electrical properties of PVA–LiCF3SO3polymer electrolyte" Journal of Non-Crystalline Solids 356 (2010) 2277-2281

[50] M. Hema, S. Selvasekerapandian, A. Sakunthala, D. Arunkumar, H. Nithya "Structural, vibrational and electrical characterization of PVA–NH4Br polymer electrolyte system" Physica B 403 (2008) 2740 –2747

[51] M. Sivakumar, R. Subadevi, S. Rajendran, N.-L. Wu, J.-Y. Lee "Electrochemical studies on [(1−x)PVA–xPMMA] solid polymer blend electrolytes complexed with LiBF4" Materials Chemistry and Physics 97 (2006) 330–336

[52] Y. Wan, K. A.M. Creber, B. Peppley, V. T. Bui "Ionic conductivity of chitosan membranes" Polymer 44 (2003) 1057–1065

[53] F. A. Abdel-Wahab, M. Abdel-Baki "Electrical conduction and dielectric properties of lithium aluminum silicate glasses doped with Cr3+ions" Journal of Non-Crystalline Solids 355 (2009) 2239–2249

[54] I. Bekri-Abbes, E. Srasra "Characterization and AC conductivity of polyaniline–montmorillonite nanocomposites synthesized by mechanical/chemical reaction" Reactive & Functional Polymers 70 (2010) 11-18

[55] S. B. Aziz, Z. H. Z. Abidin "Electrical and morphological analysis of chitosan: AgTf solid electrolyte" Materials Chemistry and Physics 144 (2014) 280-286

[56] S. B. Aziz, O. Gh Abdullah, M. A Rasheed "Structural and electrical characteristics of PVA:NaTf based solid polymer electrolytes: role of lattice energy of salts on electrical DC conductivity" Journal of Materials Science: Materials in Electronics 28 (2017) 12873–12884

[57] B. Louati, F. Hlel, K. Guidara "Ac electrical properties and dielectric relaxation of the new mixed crystal (Na0.8Ag0.2)2PbP2O7" Journal of Alloys and Compounds 486 (2009) 299–303

[58] S. B. Aziz, O. Gh Abdullah, M. A. Rasheed, H. M. Ahmed "Effect of High Salt Concentration (HSC) on Structural, Morphological, and Electrical Characteristics of Chitosan Based Solid Polymer Electrolytes" Polymers 2017, 9(6), 187; doi:10.3390/polym9060187

[59] S. B. Aziz, T. J. Woo, M. F. Z. Kadir, H. M. Ahmed "A conceptual review on polymer electrolytes and ion transport models" Journal of Science: Advanced Materials and Devices xxx (2018) 1-17, https://doi.org/10.1016/j.jsamd.2018.01.002